telling us nothing about the physical origin of the excess topography but confirming the view that the body should reorient to the lowest energy state. This makes sense if the topography is positively correlated with the geoid. One way of producing the small GTR suggested here is to have a compensation at depth D that nearly cancels the gravity of the surface mass anomaly. The predicted GTR is then reduced from that given above by a factor $f = 1 - (1 - D/R)^3$. The data suggest $f \sim 0.1$ and this requires $D \sim 100$ km, but with a large uncertainty. There are many possible interpretations of this result. It might correspond to the base of the cold ice lithosphere. It could be a thermal anomaly on the order of 10 K, corresponding to a density anomaly of one part in a thousand extending over a depth range of 100 km (because this would be equivalent to the mass of 100 m of ice). If this arose from convection, it would argue against a thin outer convective shell. However, the geoid anomalies arising from convection do not necessarily correspond to a simple estimate of density anomalies alone (i.e., thermal isostasy) and depend on the viscosity structure. The compensation could correspond to a density anomaly in the deeper region (the mixture of ice and rock), but this seems less likely given the depth of ~500 km to the core. The compensation could be a structure that develops at depth because of a physical process that creates topography at the surface, or it could be a structure that forms at depth, causing the surface to deform. The only firm conclusion that seems possible at present is that the extent of compensation is not consistent with a cold interior that supports loads over geologic time scales.

As has been suggested for Callisto, the proposed incomplete differentiation of Titan may have arisen because of a long accretion time (on the order of 1 million years), perhaps because both bodies are at a large distance from the parent planet, as measured in units of planet radii.

References and Notes

1. J. I. Lunine, R. D. Lorenz, *Annu. Rev. Earth Planet. Sci.* **37**, 299 (2009).
2. R. A. Jacobson *et al.*, *Astron. J.* **132**, 2520 (2006).
3. N. Rappaport *et al.*, *Icarus* **126**, 313 (1997).
4. We use the rotational parameter $q_r = \omega^2 R_t^3 / GM_t = 3.9555 \times 10^{-5}$, where ω, R_t, and M_t are Titan's spin rate, radius, and mass.
5. The shape of the ellipsoid is given by $r_{ell}(\lambda,\varphi) = \frac{abc}{\sqrt{(bc\cos(\varphi)\cos(\lambda))^2 + (ca\cos(\varphi)\sin(\lambda))^2 + (ab\sin(\varphi))^2}}$, where φ is the latitude and λ is the longitude.
6. C. D. Murray, S. F. Dermott, *Solar System Dynamics* (Cambridge Univ. Press, Cambridge, 1999).
7. H. Zebker *et al.*, *Science* **324**, 921 (2009).
8. W. A. Heiskanen, H. Moritz, *Physical Geodesy* (Institute of Physical Geodesy, Technical University, Graz, Austria, 1979).
9. The associated uncertainties do not account for the limitations of the Radau-Darwin model or for the small nonhydrostatic contributions to J_2 and C_{22} and have to be regarded as purely formal. See SOM for additional discussion.
10. A. P. Showman, R. Malhotra, *Science* **286**, 77 (1999).
11. The MoI factors for Ganymede and Callisto were also obtained from the Radau-Darwin equation, from a gravity field forced to the hydrostatic ratio.
12. C. Sotin *et al.*, in *Titan from Cassini-Huygens*, R. H. Brown, J.-P. Lebreton, J. Hunter Waite, Eds. (Springer, New York, 2009), pp. 61–73.
13. A. C. Barr, R. M. Canup, *Icarus* **198**, 163 (2008).
14. A. D. Fortes, P. M. Grindrod, S. K. Trickett, L. Vočadlo, *Icarus* **188**, 139 (2007).
15. P. M. Grindrod *et al.*, *Icarus* **197**, 137 (2008).
16. W. M. Kaula, *Theory of Satellite Geodesy* (Blaisdell, Waltham, MA, 1966).

17. The work of L.I., P.R., and P.T. was funded in part by the Italian Space Agency. The work of N.J.R., R.A.J., J.W.A., and S.W.A. was carried out at the Jet Propulsion Laboratory, California Institute of Technology, under a contract with NASA. D.J.S. acknowledges support from NASA's planetary geology and geophysics program.

Supporting Online Material

www.sciencemag.org/cgi/content/full/327/5971/1367/DC1
Materials and Methods
Figs. S1 to S3
Table S1
References and Notes

28 September 2009; accepted 5 January 2010
10.1126/science.1182583

Plumage Color Patterns of an Extinct Dinosaur

Quanguo Li,[1] Ke-Qin Gao,[2] Jakob Vinther,[3,4]* Matthew D. Shawkey,[5] Julia A. Clarke,[6] Liliana D'Alba,[5] Qingjin Meng,[1] Derek E. G. Briggs,[3,4] Richard O. Prum[4,7]

For as long as dinosaurs have been known to exist, there has been speculation about their appearance. Fossil feathers can preserve the morphology of color-imparting melanosomes, which allow color patterns in feathered dinosaurs to be reconstructed. Here, we have mapped feather color patterns in a Late Jurassic basal paravian theropod dinosaur. Quantitative comparisons with melanosome shape and density in extant feathers indicate that the body was gray and dark and the face had rufous speckles. The crown was rufous, and the long limb feathers were white with distal black spangles. The evolution of melanin-based within-feather pigmentation patterns may coincide with that of elongate pennaceous feathers in the common ancestor of Maniraptora, before active powered flight. Feathers may thus have played a role in sexual selection or other communication.

Exceptionally preserved specimens from the Lower Cretaceous of China have shown that simple body contour feathers and elongate pennaceous forelimb and tail feathers, bearing both barbs and barbules, were present in basal maniraptoran dinosaurs before powered flight evolved (*1*–*3*). Discoveries of elongate leg and foot feathering in Paraves (*4*–*6*) have raised new questions about the evolutionary origin of aerodynamic feather function (*2*, *3*). Preserved color patterns have also been noted, such as the light and dark regions in the tail of *Caudipteryx* (*1*), but there has been no evidence to indicate how such patterns, or color more generally, evolved.

Fossil avian feathers preserve the morphologies of melanosomes, the melanin-containing organelles that determine key aspects of color (*7*, *8*). A recent study (*9*) reported melanosome impressions in Cretaceous feathers, but the limited sample of small regions of distinct animals and comparison on the basis of gross melanosome shape prevented the interpretation of overall plumage color patterns. Here, we analyze melanosome size, shape, density, and distribution in order to reconstruct the plumage color patterns of a new specimen of a feathered dinosaur. The specimen, BMNHC PH828 (*10*) (Figs. 1 and 2 and figs. S3 and S4), comprises part and counterpart of a partial skeleton in three shale blocks, with elements of the forelimbs and distal hindlimbs in near-complete articulation. Preparation was minimal, and most feathers are well preserved even to their insertions (fig. S4). Elongate pennaceous forelimb (primaries, secondaries, and coverts) and hindlimb feathers are present, as are contour feathers associated with the skull and body (Figs. 1 and 2 and figs. S3 and S4). The new specimen is referred to *Anchiornis huxleyi* Xu *et al.* (*11*) and preserves morphologies that are consistent with the recovered placement of this species within Paraves as a part of Troodontidae [supporting online material (SOM) text] (*6*). It was found in strata estimated to be Late Jurassic in age from the Daxishan site (Jianchang County, Liaoning Province), which

[1]Beijing Museum of Natural History, 126 Tianqiao South Street, Beijing 100050, People's Republic of China. [2]School of Earth and Space Sciences, Peking University, Beijing 100871, People's Republic of China. [3]Department of Geology and Geophysics, Yale University, New Haven, CT 06511, USA. [4]Peabody Museum of Natural History, Yale University, New Haven, CT 06511, USA. [5]Department of Biology and Integrated Bioscience Program, University of Akron, Akron OH 44325-3908, USA. [6]Department of Geological Sciences, University of Texas at Austin, 1 University Station C1100, Austin, TX 78712, USA. [7]Department of Ecology and Evolutionary Biology, Yale University, New Haven, CT 06511, USA.

*To whom correspondence should be addressed. E-mail: jakob.vinther@yale.edu

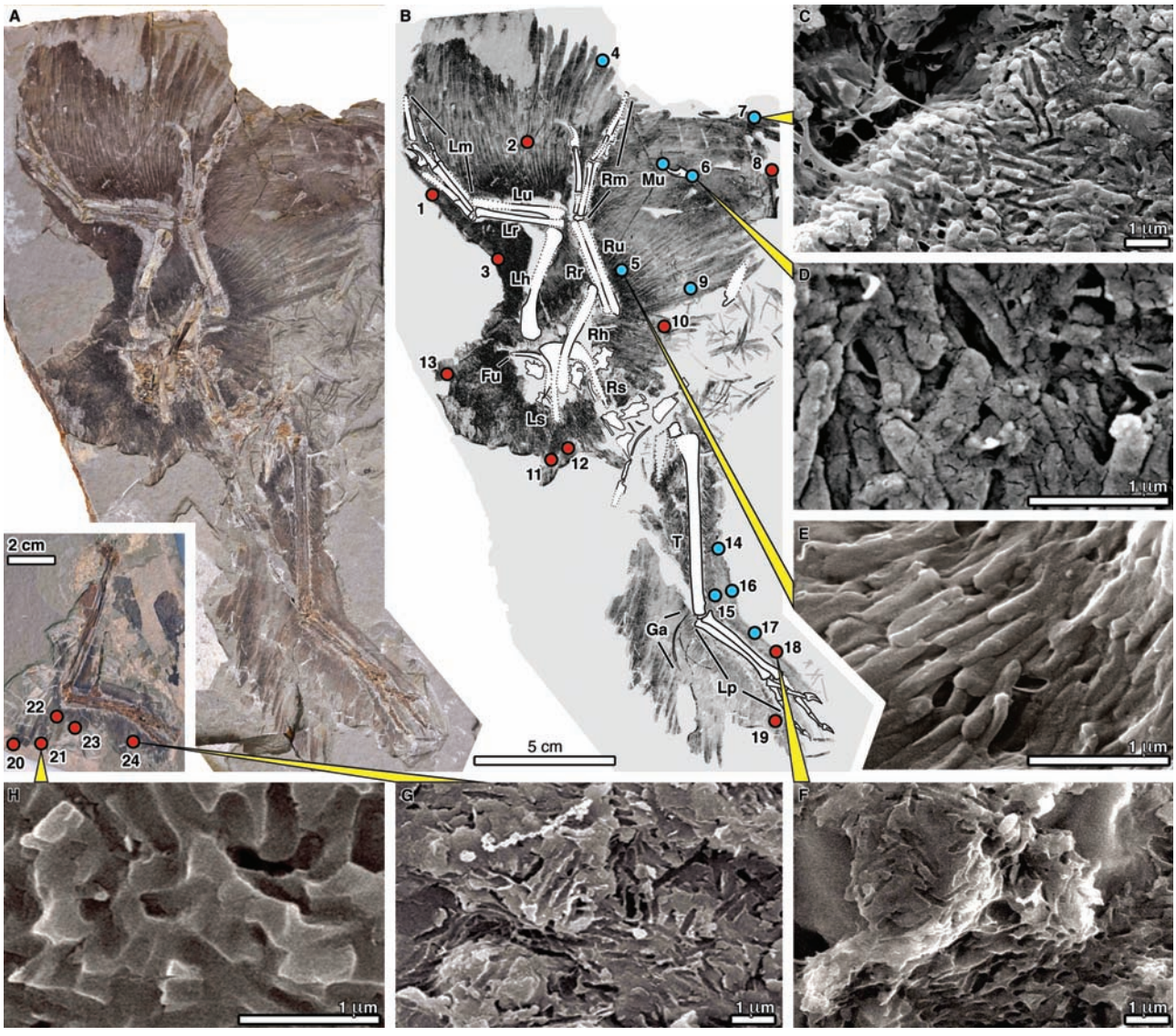

Fig. 1. *A. huxleyi* (BMNHC PH828) with SEMs of samples from the feathers. (**A**) Part, with inset of isolated right hindlimb. The left forelimb is seen in ventral view, and the right is seen in dorsal view. (**B**) Explanatory illustration. Numbered dots indicate samples from the part (red) and counterpart (blue) (table S4 and fig. S5). (**C** to **H**) SEMs of melanosomes and melanosome impressions taken from samples 7 (C), 6 (D), 5 (E), 18 (F), 24 (G), and 21 (H). Ga, gastralia; Fu, furcula; Lh, left humerus; Lm, left manus; Lp, left pes; Lr, left radius; Ls, left scapula; Lu, left ulna; Mu, manual ungual; Rh, right humerus; Rm, right manus; Rr, right radius; Ru, right ulna; Rs, right scapula.

is the same locality as a specimen recently referred to this taxon (LPM-B00169) (*6*).

We sampled proximal and distal parts of all feather types and all body regions preserved in BMNHC PH828 (Figs. 1 and 2 and table S4). Scanning electron micrographs (SEMs) of all 29 samples revealed impressions of spherical to oblate carbonaceous bodies or impressions 100 to 1908 nm in length (Figs. 1 and 2 and fig. S2) identified as melanosomes (*8*). Most samples revealed elongate eumelanosomes that varied slightly in morphology and distribution in different regions of the body. The distal crown feathers contained distinct subspherical phaeomelanosomes ~500 nm in length (Fig. 2B). A posteroventral sample from the skull showed distinct regions of spherical and elongate melanosomes.

For comparison, we assembled a data set on melanosomes from a phylogenetically diverse sample of extant bird feathers with black, gray, and brown melanin pigmentation but lacking structural coloration (*12*). Other molecular pigments, such as carotenoids and porphyrins, also produce plumage colors but are not preserved morphologically; thus, we cannot address their possible effects here. Four properties of melanosome morphology and distribution—long axis variation, short axis skew, aspect ratio, and density—were used as variables in a canonical discriminant analysis (table S1) (*12*). In general, eumelanosomes that produce black and gray colors are long and narrow, whereas those that produce rufous red and brown colors are short and wide (SOM text). We assigned colors to the fossil samples on the basis of the discriminant analysis of modern feather colors (Fig. 3 and fig. S1). All the melanosome morphologies in the fossil fell within the range of those observed in extant birds (fig. S2). Twenty-four samples were assigned a color with >0.9 probability (table S4). Three samples were ambiguous, with probabilities between 0.56 and 0.74, and three samples lacked significant numbers of melanosomes and were interpreted as unpigmented (table S4) (*8*). Sample 14 is a distinct outlier in the analysis, probably because of its high aspect ratio and long axis variation, and was predicted as gray.

Although melanosome morphologies for black and brown are strongly diagnostic, a variety of melanosome morphologies and densities generate gray colors (SOM text, tables S2

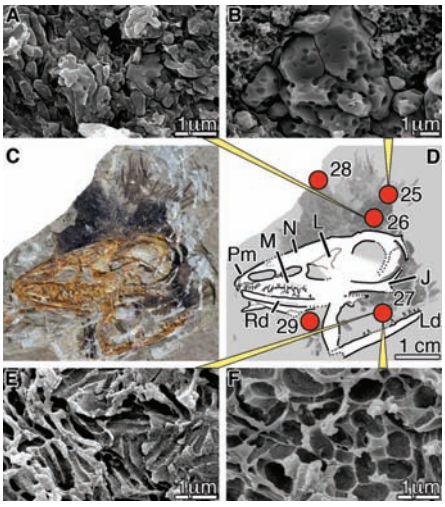

Fig. 2. *A. huxleyi* (BMNHC PH828) isolated skull with SEMs of samples from the feathers. (**C**) Skull. (**D**) Explanatory illustration. Numbered dots indicate samples. J, jugal; L, lacrimal; Ld, left dentary; M, maxillare; N, nasale; Pm, premaxillare; Rd, right dentary. (**A**, **B**, **E**, and **F**) SEMs of samples 26 (A), 25 (B), and 27 (E) and (F).

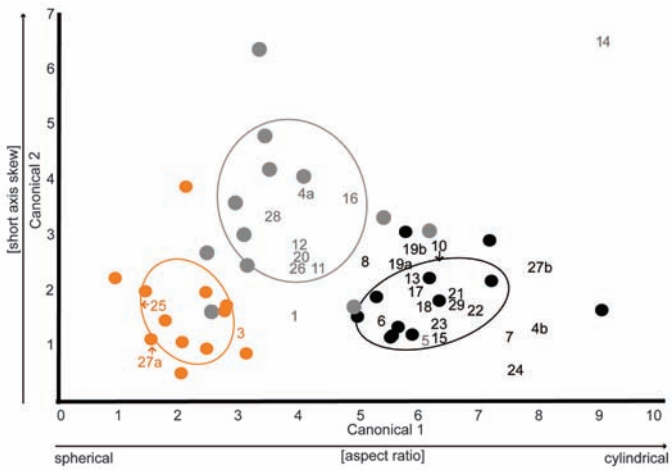

Fig. 3. Quadratic discriminant analysis of color (black, brown, or gray) in extant birds (dots) and in samples from BMNHC PH828 (numbers). The analysis identified properties of melanosome morphology and distribution that predicted color in extant birds and then used these data to predict colors in the fossil sample (fig. S1, and tables S1 to S4) (*12*). Canonical axis 1 is strongly positively associated with melanosome aspect ratio, and axis 2 is strongly positively associated with melanosome density skew. When present, arrows point to the locations of the samples in canonical space; this was done to avoid overlap of sample names.

and S3, and fig. S1). Samples from body contour feathers (samples 10 to 13) indicate a black or gray color (Fig. 3 and table S4). Samples from the marginal forelimb coverts (samples 1 and 5) and the front and dorsal surface of the legs (samples 14 to 16 and 18) were also black or gray. The undercoverts in the propatagial region were predicted as brown (table S4), albeit with low probability (0.7). Samples from the distal tips of the elongate primary and secondary feathers of the forelimb (samples 4 and 6 to 8), the toes (sample 19), and the elongate pennaceous feathers of the pedal surface of the shank (tibia) and foot (samples 20 to 24) were reconstructed as black. Melanosomes in sample 17 are poorly preserved, preventing the interpretation of color. A heterogeneous sample from the contour feathers on the side of the face (sample 27) showed separate regions of distinct melanosomes and was reconstructed as containing distinct, adjacent black and rufous feathers or parts of feathers. Samples from the long forecrown feathers and the shorter feathers from the sides of the crest (samples 28 and 26) indicate gray, whereas the longest feathers from the center of the crest (sample 25) indicate a brown in close proximity to rufous. The discriminant analysis clustered sample 25 with rufous feathers of living birds. Melanosomes were sparse in basal portions of the elongate pennaceous feathers of the forelimb and the hindlimb (samples 2, 9, and 15), indicating that these areas were lightly pigmented and whitish in color (*8*). The correlation between the colors reconstructed on the basis of melanosome morphology and density and the preserved appearance of the fossil (*8*) supports extrapolation of at least dark and light color patterning (SOM text); for example, part and

Fig. 4. Reconstruction of the plumage color of the Jurassic troodontid *A. huxleyi.* The tail is unknown in specimen BMNHC PH828 and reconstructed according to the complete specimen previously described (*6*). Color plate is by M. A. DiGiorgio.

counterpart of the *Anchiornis* specimen exhibit dark tips on many of the upper covert feathers of the forelimb and the hindlimb that are consistent with eumelanin pigmention (fig. S4, A and D).

A. huxleyi was darkly colored with gray and black body plumage (Fig. 4). The head was gray and mottled with rufous and black. Elongate gray feathers on the front and sides of the crest appear to frame a longer rufous hindcrown. Gray marginal wing coverts formed a dark epaulet that contrasted strongly with the black- and gray-spangled light primaries, secondaries, and greater coverts of the forelimb. The large black spangles of the primaries and secondaries created a dark outline to the trailing edge of the forelimb plumage. The spangles of the outermost primaries were black. The greater coverts of the upper wing were spangled with gray or black, creating an array (secondary coverts) or rows (primary coverts) of conspicuous dots. The contour feathers of the legs were gray on the shank and black on the foot. Like the forelimb, the elongate feathers of the lateroplantar surface of the hindlimb were white at their bases with broad black distal spangles. The tail is unknown in BMNHC PH828.

The plumage color pattern elements of the Late Jurassic *A. huxleyi* are strikingly similar to various living birds, including domesticated fowl, providing insights into the evolution of feather-pigment pattern development (SOM text). The identification of melanin-based within- and among-feather plumage coloration patterns in *Anchiornis* helps reveal the evolution of color pigmentation patterning mechanisms in dinosaurs. For example, the pattern observed in the simple tail integumentary structures of the basal coelurosaur *Sinosauropteryx prima* (*13*) has been interpreted as representing spaced light and dark patches among feathers. Our results confirm that

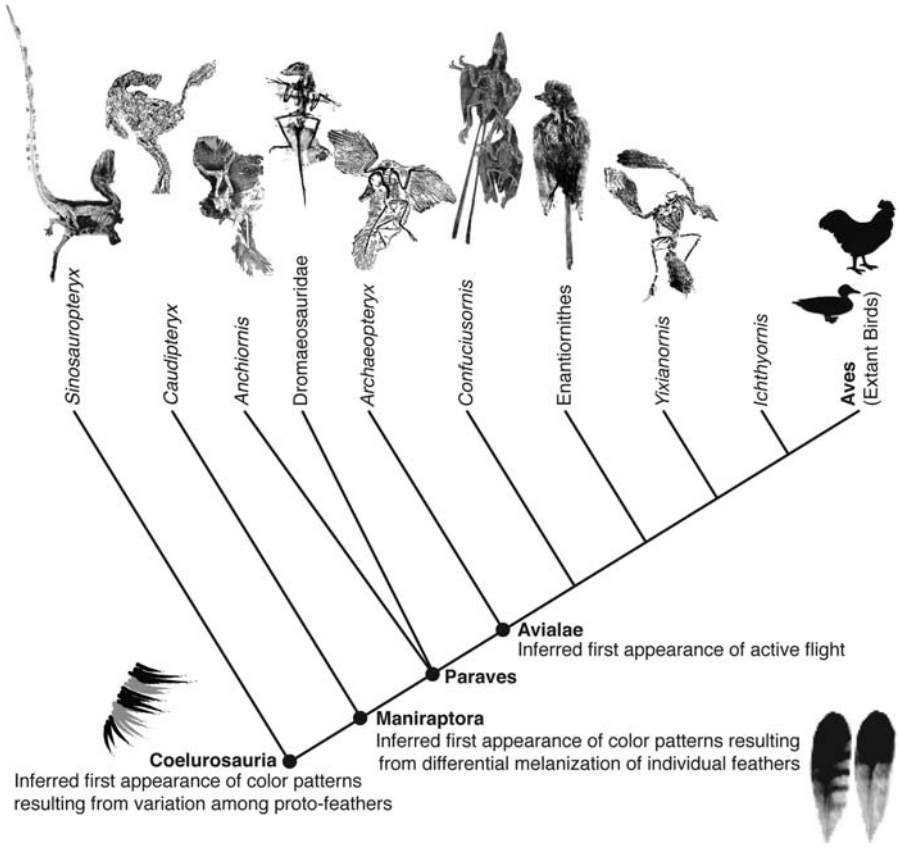

Fig. 5. The distribution of integumentary types in coelurosaurian theropod dinosaurs and inferred distribution of plumage patterning (*2*, *3*, *6*). Protofeather-like appendages appeared at the base of Coelurosauria, if not earlier (*3*). Color patterns reported in the tail of the compsognathid *Sinosauropteryx* (*9*) indicate that among-feather color patterns may have also appeared at this stage. Pinnate feathers and within-feather color patterns first appear in Maniraptora, as observed in the striped pinnate tail feathers of the oviraptorosaur *Caudipteryx* (*1*, *20*, *21*) and the troodontid *A. huxleyi*.

melanin-based patterning is a mechanism for within- and among-feather variation, producing lighter and darker regions. According to our data from *Anchiornis* and its phylogenetic placement (*6*), these two common mechanisms of plumage patterning in crown group Aves are supported as minimally having a first appearance in the most recent common ancestor of Troodontidae + crown Aves. Further, although paravian relationships remain controversial, recent analyses recover a monophyletic Deinonychosauria (*6*, *14*), indicating support for within- and among-feather variation as ancestral to at least Paraves (Fig. 5).

Complex within- and among-feather plumage coloration, such as that in *A. huxleyi*, is used in display and communication in living birds. Such communication, however, may function in different ways: commonly in intersexual communication (*15*), and less so in interspecific and intraspecific competition for restricted foraging [for example, multiple species of antbirds forage on army ant swarms (*16*)]. Alternatively, bold plumage color patterns can function in interspecific threat and defense postures [such as in some owls or the sunbittern (*Eurypygia helias*)], in startling predators or warning conspecifics within a flock (*17*), or in startling invertebrate prey that are seized as they attempt to flee (such as with North American *Setophaga* redstarts, Neotropical *Myioborus* whitestarts, and Australian *Rhipidura* fantails) (*18*, *19*). Melanin deposition in the distal portion of primaries in birds such as gulls (Laridae) may offer added resistance to wear (*20*).

The plumage of *Anchiornis* is composed of a variety of differently sized pennaceous (closed-vaned and rachidial) feathers that vary little in feather shape (Fig. 1 and figs. S3 and S4). The body contour feathers, the primary and secondary forelimb feathers, and the forelimb and hindlimb coverts all share a similar aspect ratio (length to width). Thus, mechanisms producing varieties of feather shape may postdate the evolutionary first appearance of plumage color variation (SOM text).

The most recent common ancestor of *Anchiornis* and Aves must have had the capacity to develop white, gray, black, and rufous plumage color patterns both within and among feathers. Both mechanisms of melanin-based plumage patterning evolved before the derived form of active powered flight minimally inferred as ancestral to Avialae (Fig. 5). The observed color pattern in *Sinosauropteryx* is consistent with only among-feather variation in melanin pigment deposition. Such variation occurs in Aves and would be optimized as ancestral to at least Coelurosauria (Fig. 5). However, the evolutionary origin of within-feather pigmentation patterning, including stripes, feather spots, and spangles, appears phylogenetically later. Its origin is presently coincident with the origin of elongate pennaceous feather structure in the most recent common ancestor of Maniraptora when data from *Caudipteryx* (*1*, *10*, *20*) are considered (Fig. 5). Thus, the first evidence for plumage color patterns in a feathered nonavian dinosaur suggests that selection for signaling function may be important in the early evolution of feathers.

References and Notes

1. Q. Ji, P. J. Currie, M. A. Norell, S.-A. Ji, *Nature* **393**, 753 (1998).
2. M. A. Norell, X. Xu, *Annu. Rev. Earth Planet. Sci.* **33**, 277 (2005).
3. X. Xu, Y. Guo, *Vertebrata PalAsiatica* **47**, 311 (2009).
4. F. Zhang, Z. Zhou, *Nature* **431**, 925 (2004).
5. X. Xu *et al.*, *Nature* **421**, 335 (2003).
6. D. Hu, L. Hou, L. Zhang, X. Xu, *Nature* **461**, 640 (2009).
7. J. Vinther, D. E. G. Briggs, J. Clarke, G. Mayr, R. O. Prum, *Biol. Lett.* **6**, 128 (2010).
8. J. Vinther, D. E. G. Briggs, R. O. Prum, V. Saranathan, *Biol. Lett.* **4**, 522 (2008).
9. F. Zhang *et al.*, *Nature*; published online 27 January 2010 (10.1038/nature08740).
10. Z. Zhou, X. Wang, *Vertebrata PalAsiatica* **38**, 113 (2000).
11. X. Xu *et al.*, *Chin. Sci. Bull.* **54**, 430 (2009).
12. Materials and methods are available as supporting material on *Science* Online.
13. Q. Ji, S. Ji, *Chin. Geol.* **23**, 30 (1996).
14. A. H. Turner, D. Pol, J. A. Clarke, G. M. Erickson, M. A. Norell, *Science* **317**, 1378 (2007).
15. G. E. Hill, K. J. McGraw, Eds., *Bird Coloration*, vol. 2, *Function and Evolution* (Harvard Univ. Press, Cambridge, MA, 2006).
16. S. K. Willson, *Ornithol. Monogr.* **55**, 1 (2004).
17. G. R. Bortolotti, in *Bird Coloration*, vol. 2, *Function and Evolution*, G. E. Hill, K. J. McGraw, Eds. (Harvard Univ. Press, Cambridge, 2006), pp. 3–35.
18. P. G. Jablonski, *Behav. Ecol.* **10**, 7 (1999).
19. R. L. Mumme, *Auk* **119**, 1024 (2002).
20. E. H. Burtt Jr., in *The Behavioral Signification of Color*, E. H. Burtt Jr., Ed. (Garland STPM Press, New York, 1979) pp. 75–110.
21. Z. Zhou, X. Wang, F. Zhang, X. Xu, *Vertebrata PalAsiatica* **38**, 241 (2000).

22. E. Champion and S. Nesbitt helped produce the figures. N. Vitek, J. A. Cundiff, and C. L. Canter made initial investigations of modern feathers. The research was funded by NSF (EAR-0720062 and EAR-0719758), the Air Force Office of Scientific Research (FA9550-09-1-0159), University of Akron startup funds, the National Geographic Society, and the Yale University W. R. Coe Fund. K. J. McGraw and R. J. Safran provided modern feather samples. The studied specimen is accessioned at Beijing Museum of Natural History (BMNHC). The color plate in Fig. 4 was painted by M. D. DiGiorgio.

Supporting Online Material

www.sciencemag.org/cgi/content/full/science.1186290/DC1
Materials and Methods
SOM Text
Tables S1 to S5
Figs. S1 to S5
References

22 December 2009; accepted 25 January 2010
Published online 28 January 2010;
10.1126/science.1186290
Include this information when citing this paper.